The effect of pressure on the electronic states of FeS and Fe_7S_8 studied by Mössbauer spectroscopy

1997 J. Phys.: Condens. Matter 9 515

(http://iopscience.iop.org/0953-8984/9/2/019)

J. Phys.: Condens. Matter **9** (1997) 515–527. Printed in the UK PII: S0953-8984(97)76655-4

The effect of pressure on the electronic states of FeS and Fe_7S_8 studied by Mössbauer spectroscopy

Hisao Kobayashi†§, Masaki Sato†, Takashi Kamimura†, Masamichi Sakai‡, Hideya Onodera‡, Noritaka Kuroda‡ and Yasuo Yamaguchi‡

† Department of Physics, Tohoku University, Sendai, 980-77, Japan

‡ Institute for Materials Research, Tohoku University, Sendai, 980-77, Japan

Received 24 July 1996, in final form 23 October 1996

Abstract. We have measured under pressure ^{57}Fe Mössbauer spectra of FeS and 3*c*-type Fe_7S_8 up to 16 GPa and x-ray diffraction patterns of Fe_7S_8 up to 11 GPa at room temperature. It is found for Fe_7S_8 that the compressibilities of the lattice parameters exhibit definite anomalies at around 4.5 GPa and that there is no change in the crystal structure up to 11 GPa. Magnetically ordered Mössbauer spectra are observed below 6.5 GPa for FeS and 4.5 GPa for Fe_7S_8, whereas the spectra above these pressures are typical of a paramagnetic ordering with a quadrupole splitting. A large reduction in the centre shift is observed at these pressures. It is found that there is a distinct steplike feature of the magnetic hyperfine field at 3.5 GPa for FeS. The electronic states of FeS and Fe_7S_8 are deduced from the volume dependences of the centre shift and the magnetic hyperfine field. Below 3.5 GPa for FeS, the electronic state has an insulating character and the electrons on the iron are well localized and thus contribute to the magnetic moment. In the intermediate-pressure range, from 3.5 to 6.5 GPa for FeS and below 4.5 GPa for Fe_7S_8, the electronic state is like a semimetallic one. Above 6.5 GPa for FeS and 4.5 GPa for Fe_7S_8, the electronic bandwidth is large enough to cause the state to become metallic and produces a collapse of the iron magnetic moment.

1. Introduction

The electronic properties of 3d-transition-metal compounds, where an electron correlation plays an important role, have been viewed as an interesting subject, especially since the discovery of high-T_c superconductors. One of the interesting properties in these compounds is an insulator–metal transition. Before the discovery of the high-T_c superconductors, the nature of this transition was investigated using the Mott–Hubbard theory in which the d–d Coulomb interaction is larger than the one-electron dispersional part of the bandwidth. Zaanen, Sawatzky, and Allen (ZSA) have developed a general framework for these compounds [1]. According to the ZSA scheme, the transition metal compounds can be classified into regimes based on the relative magnitudes of the ligand-to-metal charge-transfer energy, Δ, the on-site Coulomb energy, U, and the bandwidth. There are two general types of gap possible: the Mott–Hubbard gap due to U and the charge-transfer gap due to Δ. FeS is believed to belong to the intermediate regime, where $\Delta \leqslant U$ and U is not very large.

Iron sulphide has a substantial deficiency at the iron site. In the range $0 \leqslant x \leqslant 0.15$ of the system $Fe_{1-x}S$, two compounds were reported: a troilite ($x \sim 0$) and a pyrrhotite

§ Author to whom any correspondence should be addressed; fax: +8122-263-9278; e-mail: kobayash @susy.kaws.coge.tohoku.ac.jp.

0953-8984/97/020515+13$19.50

(x around 0.125). For ambient conditions, stoichiometric FeS has the troilite crystal structure which is closely related to the NiAs-type structure, and is an antiferromagnet with $T_N = 598$ K [2]. As indicated by high-pressure x-ray diffraction measurements [3, 4], it undergoes two successive first-order phase transitions with increasing pressure at room temperature. The first transition occurs at 3.5 GPa and the structure transforms to a MnP-type one. The second transition takes place at 6.5 GPa with about 10% volume reduction, although its structure is uncertain. The measurement of ^{57}Fe Mössbauer spectra was carried out under pressure up to about 15 GPa [5]. At low pressure the spectra consist of six peaks whereas at high pressure the spectrum is typical of paramagnetic irons. However, the electronic properties of FeS have never been clear in high-pressure phases. $Fe_{0.875}S$ is a ferrimagnet with $T_c = 578$ K [6] and the fundamental crystal structure is the NiAs-type one, where one eighth of the iron sites are vacant and the composition can be represented as Fe_7S_8. Two types of superstructure due to the ordering of vacancies are known of [7, 8]; one is a hexagonal superstructure (3c structure) and the other is a monoclinic superstructure (4c structure). Quenching from 500 °C produces the 3c structure and slow cooling yields the 4c structure. It was observed from high-pressure x-ray diffraction measurements at room temperature [4] that the compressibilities of lattice parameters exhibit definite anomalies at 6.2 GPa for the 4c structure. Neither volume nor structure was observed to change at this pressure.

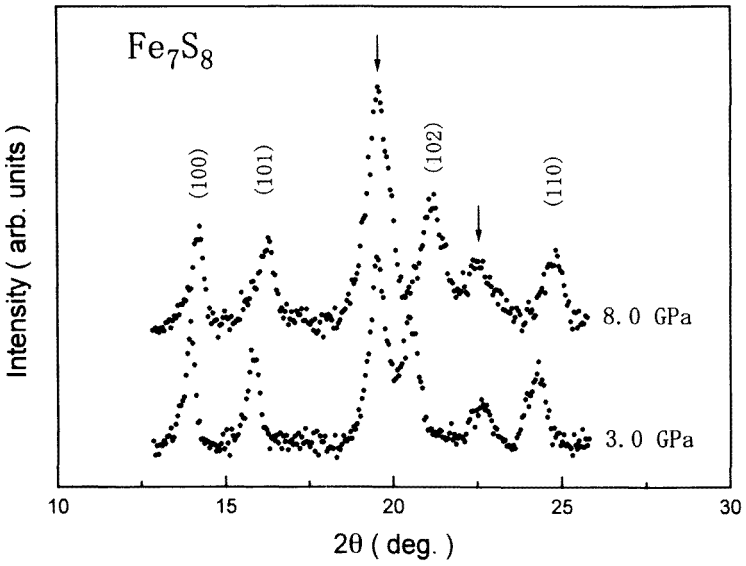

Figure 1. X-ray diffraction patterns of the 3c-Fe_7S_8 at 3.0 and 8.0 GPa obtained using Mo Kα radiation. The arrows indicate diffraction lines from the Inconel 625 gasket. The other diffraction lines are indexed with respect to the NiAs-type unit cell.

According to our low-temperature specific heat measurement [9], the electronic specific heat coefficients, γ, for FeS and $Fe_{0.875}S$ are estimated to be 0.01 ± 0.1 and 14.88 ± 0.06 mJ K^{-2} mol^{-1}, respectively. The photoemission and inverse photoemission spectroscopy [10] indicated that the observed intensity at the Fermi level of FeS is weak, while that of $Fe_{0.875}S$ is strong. The previous resistance measurements at ambient pressure showed that FeS has a slightly decreasing resistance with increasing temperature and that the resistance

of $Fe_{0.875}S$ remains almost constant as the temperature is varied [11, 12]. These results indicate that the ground state of FeS should be an insulating one and that the gap should go to zero for $Fe_{0.875}S$.

Mössbauer spectroscopy is a useful method for the study of electronic properties of materials under very high pressure [13]. In the present study, we have carried out ^{57}Fe Mössbauer effect and x-ray diffraction measurements on FeS and 3*c*-type Fe_7S_8 under high pressure and reported the dependences of the lattice parameters on pressure and the hyperfine interaction parameters on volume. We discuss the electronic states of FeS and Fe_7S_8 under pressure.

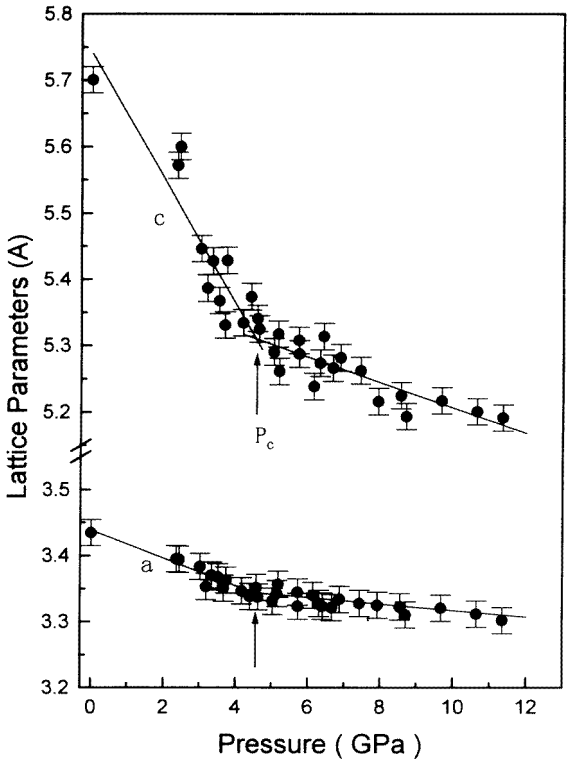

Figure 2. Pressure dependences of the lattice parameters, *a* and *c*. The solid lines represent the fitting results, assuming linear pressure dependences of *a* and *c*.

2. Experimental procedure

The polycrystalline samples were prepared using the following procedure. Appropriate amounts of the starting materials Fe (99.998% purity) and S (99.9999% purity) were sealed in an evacuated quartz tube and then were heated to 800 °C for several days; the product was ground and heated at 800 °C for several further days in an evacuated quartz tube. The sulphur vapour reacted with the iron block completely during the process. FeS was produced by slow cooling from 800 °C and the 3*c*-type Fe_7S_8 was yielded by quenching from 500 °C. The Fe_7S_8 sample is hexagonal with distinct reflections of the 3*c* type. The two $Fe_{1-x}S$ samples have the compositions $Fe_{0.999}S$ and $Fe_{0.874}S$, as determined from the

Table 1. Hyperfine interaction parameters in FeS, (a), and Fe_7S_8, (b), under pressure. ΔE_Q can be expressed as $\frac{1}{2}eV_{zz}Q(3\cos^2(\vartheta)-1)/2$ in the magnetically ordered state and $|\frac{1}{2}eV_{zz}Q(1-\eta)^{1/2}|$ in the paramagnetic state, where Q is the nuclear electric quadrupole moment, $V_{zz} = \partial^2 V/\partial^2 z$ the principal component of the diagonalized EFG, ϑ the angle between the directions of the principal axis of the EFG and the magnetic hyperfine field and $\eta = (V_{xx} - V_{yy})/V_{zz}$.

P (GPa)	δ_{CS} (mm s^{-1})	ΔE_Q (mm s^{-1})	H_{hf} (kOe)		$\Delta V/V_0$
(a)					
0.0001	0.76(1)	−0.19(2)	315(5)		0.0
0.7	0.76(1)	−0.18(2)	315(5)		0.010
2.1	0.72(1)	−0.15(2)	317(5)		0.029
2.6	0.72(1)	−0.16(2)	316(5)		0.036
3.6	0.72(1)	−0.09(2)	315(5)	0.43[a]	0.050
	0.74(1)	+ 0.25(2)	279(5)	0.57	0.067
4.3	0.71(1)	+ 0.30(2)	273(5)		0.078
4.6	0.72(1)	+ 0.30(2)	273(5)		0.082
6.3	0.69(1)	+ 0.30(2)	261(5)	0.66[a]	0.104
	0.54(1)	0.44(2)		0.34	0.190
7.4	0.55(1)	0.42(2)			0.197
8.1	0.54(1)	0.42(2)			0.201
16.0	0.40(1)	0.28(2)			0.300

x-ray diffraction measurement using the empirical relation for the (102) interplanar spacing versus the concentration of Fe in the Fe–S system [14].

High-pressure x-ray diffraction measurements were carried out at room temperature using a diamond-anvil cell (DAC) up to 11 GPa. A sample cavity was drilled in a 0.3 mm thick Inconel 625 alloy gasket with a 0.4 mm diameter, and Fe_7S_8 powders were loaded into the cavity with a ruby crystal. A 4:1 methanol–ethanol mixture was used as a pressure medium which ensured quasihydrostatic conditions. Pressure was calibrated by measuring the wavelength shift of the R_1 luminescence line of the ruby crystal irradiated by the Ar^+-ion laser. The DAC was mounted on a goniometer and diffraction patterns were collected in the Debye–Scherrer geometry using point-focus Mo Kα radiation.

The Mössbauer spectra were measured at room temperature under high pressure up to 16 GPa using a clamp-type DAC. The powdered samples were mixed with fine BN powders in order to get a uniform resonant-absorber thickness and loaded with a ruby crystal into a sample cavity of a 0.4 mm diameter in a 0.3 mm thick Inconel 625 alloy gasket. The use of Fluorinert as the pressure-transmitting medium ensured quasihydrostatic conditions. Pressure was also calibrated by measuring the wavelength shift of the R_1 luminescence line of the ruby crystal. The clamp-type DAC was mounted on a translation stage with the sample at a distance of approximately 3 mm from an 8 mCi ^{57}Co-in-Rh source with a high-space-activity area of 800 mCi cm^{-2}. The 14.4 keV γ-ray was detected with a 1 atm Kr–CO_2-filled proportional counter. The velocity scale was calibrated with α-iron at room temperature. While Mössbauer samples in high-pressure experiments are usually synthesized in such a way as to be enriched in ^{57}Fe, samples not enriched in ^{57}Fe were prepared by the method above. As seen in figure 3 later, spectra of satisfactory quality were obtained in 30–50 hours.

Table 1. Continued

P (GPa)	Intensity	δ_{CS} (mm s^{-1})	ΔE_Q (mm s^{-1})	H_{hf} (kOe)	$\Delta V/V_0$
(b)					
0.0001	2.0	0.69(1)	+ 0.05(2)	305(5)	0.0
	1.0	0.69(1)	+ 0.12(2)	295(5)	
	2.0	0.67(1)	+ 0.06(2)	256(5)	
	1.0	0.67(1)	+ 0.12(2)	234(5)	
	1.0	0.67(1)	+ 0.21(2)	221(5)	
		0.68(1)	—	268(5)	
2.3	3.0	0.64(2)	+ 0.01(4)	269(10)	0.073
	2.0	0.62(2)	+ 0.05(4)	225(10)	
	2.0	0.63(2)	+ 0.09(4)	186(10)	
		0.63(2)	—	233(10)	
2.5	3.0	0.61(2)	−0.07(4)	249(10)	0.076
	2.0	0.58(2)	+ 0.04(4)	209(10)	
	2.0	0.60(2)	+ 0.07(4)	170(10)	
		0.60(2)	—	215(10)	
3.9[b]		0.64(2)	–	102(20)	0.121
5.1	3.0	0.49(2)	0.49(4)		0.143
	2.0	0.48(2)	0.72(4)		
	2.0	0.53(2)	0.15(4)		
		0.50(2)	—		
5.4	3.0	0.50(2)	0.49(4)		0.145
	2.0	0.47(2)	0.72(4)		
	2.0	0.54(2)	0.15(4)		
		0.50(2)	—		
7.3	3.0	0.47(2)	0.48(4)		0.156
	2.0	0.46(2)	0.76(4)		
	2.0	0.51(2)	0.20(4)		
		0.48(2)	—		
8.3	3.0	0.47(2)	0.43(4)		0.161
	2.0	0.44(2)	0.81(4)		
	2.0	0.49(2)	0.22(4)		
		0.47(2)	—		
10.0	3.0	0.44(2)	0.52(4)		0.169
	2.0	0.43(2)	0.79(4)		
	2.0	0.49(2)	0.25(4)		
		0.45(2)	—		

[a] This is an intensity ratio of two subspectra.

[b] Since H_{hf} is too small for subspectra to be extracted at 3.9 GPa, the spectrum was analysed assuming the distribution of H_{hf}.

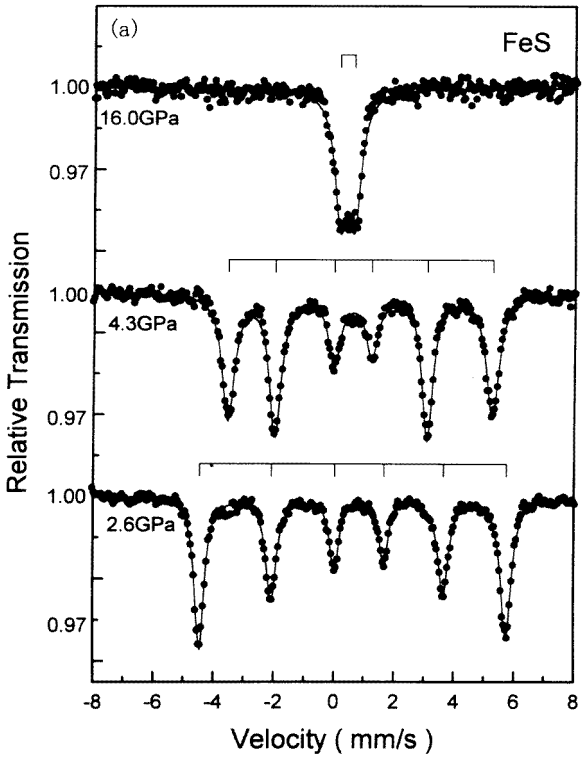

Figure 3. Mössbauer spectra under pressure of FeS, (a), and Fe_7S_8, (b). The closed circles indicate the observed spectrum, the solid line represents the fitted curve obtained by the analysis, and the extracted subspectra are shown by the bar diagrams. The relative intensities of the bar diagrams show those of the individual iron sites. The velocity scale is relative to that of α-iron.

3. Experimental results

3.1. X-ray diffraction measurements

As shown in figure 1, all observed x-ray diffraction patterns of Fe_7S_8 consist of diffraction lines of the fundamental NiAs structure. Thus no transition in a crystal structure is found up to 11 GPa within the experimental accuracy. The observed x-ray diffraction patterns were analysed using a Gaussian line shape. The lattice parameters, a and c, of the NiAs-type unit cell were obtained from d-values of these lines using the least-squares fitting method, although $3c$-Fe_7S_8 has a unit cell with $A = 2a$ and $C = 3c$. Figure 2 shows the pressure dependences of a and c. It is found that these pressure dependences of a and c exhibit definite anomalies, and no discontinuous volume change is observed at around 4.5 GPa, which is similar to the case for $4c$-type Fe_7S_8 at 6.2 GPa [4]. The anomaly suggests that the electrical and/or magnetic phase transition takes place at around 4.5 GPa. The compressibilities of a and c, κ_a and κ_c, were estimated to be $(6.1 \pm 0.9) \times 10^{-3}$ and $(16 \pm 3) \times 10^{-3}$ GPa^{-1} below 4.5 GPa, and $(1.8 \pm 0.4) \times 10^{-3}$ and $(3.5 \pm 0.4) \times 10^{-3}$ GPa^{-1} above 4.5 GPa, respectively, assuming linear pressure dependences of a and c. Since κ_c is about three times larger than κ_a below 4.5 GPa, there is a large pressure dependence of c/a. The a- and c-values above 4.5 GPa are comparable with those of Co_7S_8 [4]. The

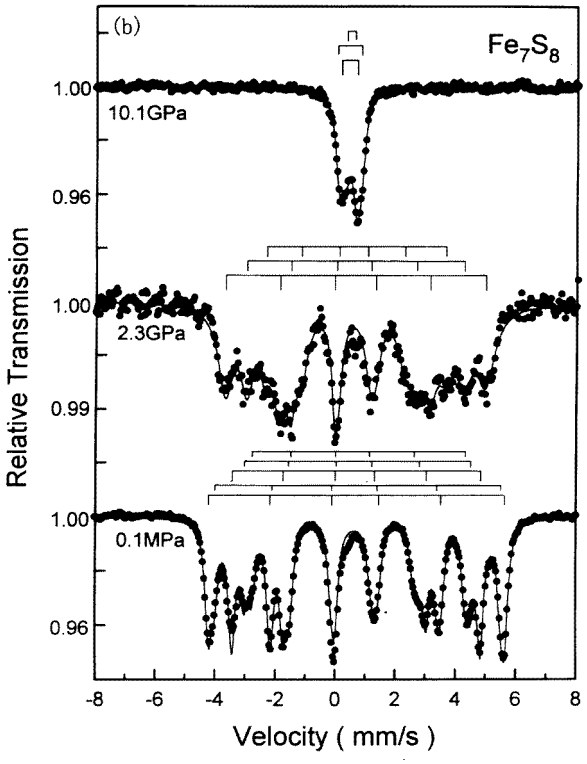

Figure 3. (Continued)

volume extrapolated to 0.1 MPa from above 4.5 GPa is estimated to be about 10% smaller than that at 0.1 MPa.

3.2. Mössbauer spectroscopy

Typical observed ^{57}Fe Mössbauer spectra for FeS and Fe_7S_8 are shown in figure 3 where the closed circles indicate the observed spectra. It is found that the spectra of FeS below 6.0 GPa mainly consist of a magnetic hyperfine field for which the electric quadrupole interaction is not very large, whereas the spectra above 6.5 GPa are typical of paramagnetism with a quadrupole splitting. It is observed that the spectra of Fe_7S_8 below 4 GPa are magnetically ordered ones and the magnetic hyperfine fields disappear above 5 GPa. Thus the transition of Fe_7S_8 at 4.5 ± 0.5 GPa has a good correspondence to that of FeS at 6.5 ± 0.5 GPa.

The observed Mössbauer spectra were analysed with a Lorentzian line shape, and the thickness broadening and geometrical effects were taken into account. In figure 3, the solid lines represent the fitted curves obtained by this analysis and the extracted subspectra are shown by the bar diagrams. The refined hyperfine interaction parameters are summarized in table 1. As shown in figure 3(a), the observed spectra of FeS were well fitted with one subspectrum in all three phases. Hence all iron atomic positions seem to be magnetically as well as crystallographically equivalent in each phase under pressure. The pressure dependence of the refined hyperfine interaction parameters for FeS shows two phase transitions at 3.5 ± 0.5 and 6.5 ± 0.5 GPa, which is in good agreement with previous work [3–5].

As shown in table 1(a), the value of $\Delta E_Q = \frac{1}{2}eV_{zz}Q(3\cos^2(\vartheta) - 1)/2$ goes from less than zero to greater than zero at 3.5 GPa, where Q is the nuclear electric quadrupole moment, $V_{zz} = \partial^2 V/\partial^2 z$ the principal component of the diagonalized electric field gradient (EFG) and ϑ the angle between the directions of the principal axis of the EFG and the magnetic hyperfine field. As indicated by high-pressure x-ray diffraction measurements on the single-crystal FeS [3], the Fe atom's coordination polyhedron does not change shape significantly up to 6.35 GPa although the structural phase transition takes place at 3.5 GPa. The quadratic elongation of the polyhedron is greater than one and goes from 1.0202 at 3.33 GPa to 1.0164 at 4.15 GPa. Thus the structural phase transition does not strongly affect the direction of the principal axis of the EFG and V_{zz}. It seems that the change of ΔE_Q at 3.5 GPa is caused by that of the direction of the iron magnetic moment, where the phase transition from the troilite to the MnP-type structure takes place.

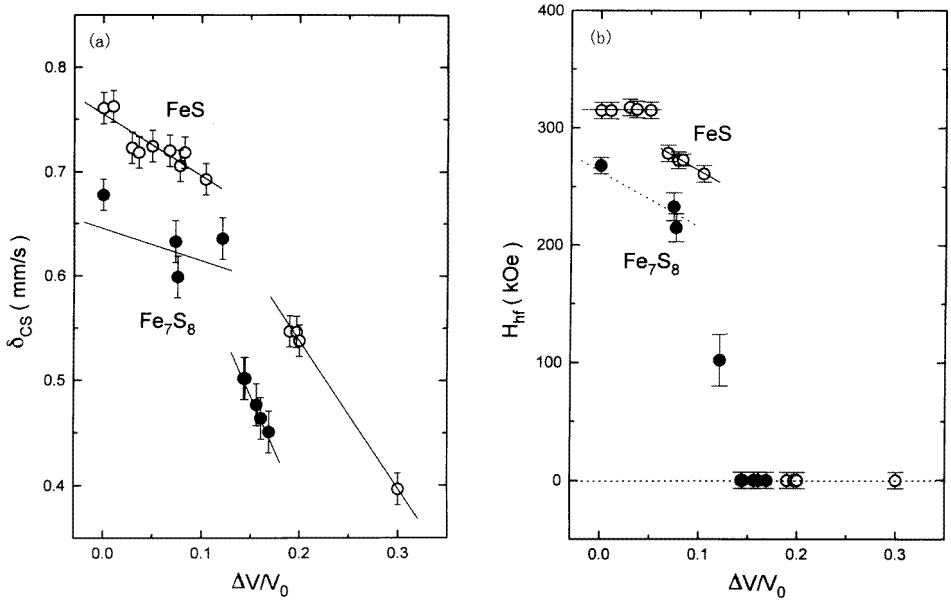

Figure 4. Variations of the centre shift, δ_{CS}, (a), and the magnetic hyperfine field, H_{hf}, (b), as functions of $\Delta V/V_0$ where $\Delta V = V(0) - V(P)$. The open and closed circles are for FeS and Fe_7S_8, respectively. The mean values of δ_{CS} and H_{hf} for different iron sites are plotted versus $\Delta V/V_0$ for Fe_7S_8. Solid lines indicate linear fits to the data. A broken line is parallel to the solid line for FeS in the range from $\Delta V/V_0$ = 0.055 to 0.11.

Nakano *et al* proposed the 3*c* structure for Fe_7S_8 on the basis of x-ray diffraction measurements [8]. The supercell is composed of twelve NiAs subcells, in which vacancies are ordered in alternating iron layers along the *c*-axis and the iron and sulphur atoms shift from the atomic positions in the ideal NiAs-type structure. According to Nakano's model, there are five crystallographically different iron sites with ratios of 2:1:2:1:1. The spectrum of Fe_7S_8 at 0.1 MPa was analysed using five subspectra with these intensity ratios and assuming the same width for all absorbing lines. The refined line width, 0.270 ± 0.005 mm s^{-1}, is comparable with the natural line width. Because of the geometrical and large broadening effects, the absorbing line widths under pressure are larger than those at 0.1 MPa. Accordingly it is difficult to discuss the fine characteristic features of the spectrum. If the atomic shift from the ideal position is ignored, these five

different iron sites are reduced to three iron sites with the ratios 3:2:2. The first site has two neighbouring vacancies in the same iron layer, and is divided into two different sites with the ratio of 2:1 in Nakano's model, the second site has one neighbouring vacancy in the iron row along the *c*-axis, and the third site has no neighbouring vacancy, and is divided into two different sites with the ratio of 1:1 in Nakano's model. The observed spectra under pressure were analysed with three subspectra assuming that the intensity ratio is as shown in figure 3(b). The refined hyperfine interaction parameters in the three iron sites had similar pressure dependences. It is observed from the pressure dependence of the hyperfine interaction parameters for Fe_7S_8 that the transition takes place from the magnetically ordered to the paramagnetic state at 4.5 ± 0.5 GPa, which is in good agreement with the result of the present high-pressure x-ray diffraction measurement.

Figure 4 shows the centre shift, δ_{CS}, and the magnetic hyperfine field, H_{hf}, for FeS and Fe_7S_8, as functions of $\Delta V/V_0$ where $\Delta V = V(0) - V(P)$ and $V(P)$ were evaluated from the present and previous high-pressure x-ray diffraction measurements [3, 4]. Mean values of δ_{CS} and H_{hf} for the different iron sites are plotted for Fe_7S_8. The values of δ_{CS} for FeS and Fe_7S_8 decrease slightly with increasing $\Delta V/V_0$ up to about 0.13. A significant change in δ_{CS} occurs at around $\Delta V/V_0 \sim 0.13$ and then δ_{CS} decreases linearly with further increase of $\Delta V/V_0$. As seen in the figure 4, there is a distinct steplike feature of H_{hf} for FeS but no observable anomaly in δ_{CS} at $\Delta V/V_0 = 0.055$. On the other hand, H_{hf} for Fe_7S_8 decreases rapidly with increasing $\Delta V/V_0$ up to about 0.13. In both FeS and Fe_7S_8, H_{hf} disappears above $\Delta V/V_0 \sim 0.13$.

4. Discussion

4.1. The bulk modulus and the volume dependence of the hyperfine interactions

The bulk moduli, B, below and above 4.5 GPa were evaluated to be 35 ± 6 and 140 ± 20 GPa, respectively, from κ_a and κ_c, using $\kappa_V = 2\kappa_a + \kappa_c$ and $B = 1/\kappa_V$. The values of B of the troilite, the MnP-type, and the higher-pressure phases of FeS were calculated to be 73, 57, and 127 GPa, respectively, from previous high-pressure x-ray diffraction measurements [3, 4]. These results show that B decreases significantly in the low-pressure phase for Fe_7S_8 and the MnP-type phase for FeS. Janak and Williams showed using self-consistent spin-polarized energy band calculations [15] that anomalously small bulk moduli of the magnetic members in the 3d transition metals are caused by the pressure deviation of the magnetic moment. Since H_{hf} depends on pressure only in the MnP-type phase for FeS and the low-pressure phase for Fe_7S_8 as shown in section 3.2, and the ground state of Fe_7S_8 at ambient pressure is predicted not to be an insulating one [9, 10], the pressure dependence of the magnetization is responsible for the small B-value of the MnP-type phase for FeS and the low-pressure phase for Fe_7S_8. As also shown by calculation [15], the difference between the values of B for the nonmagnetic and ferromagnetic states is about 100 GPa for α-iron. This value is comparable with the values of the differences for FeS and Fe_7S_8 between the values of B for the nonmagnetic and magnetic states.

The values of δ_{CS} in both FeS and Fe_7S_8 below $\Delta V/V_0 \sim 0.13$ indicate that the electronic state of iron is the high-spin Fe(II) state. Within the accuracy of the data, we obtain linear fits of the form

$$\delta_{CS} = (0.755 \pm 0.007) - (0.59 \pm 0.11)\Delta V/V_0 \text{ mm s}^{-1} \qquad \text{for FeS}$$

and

$$\delta_{CS} = (0.66 \pm 0.03) - (0.42 \pm 0.15)\Delta V/V_0 \text{ mm s}^{-1} \qquad \text{for } Fe_7S_8.$$

These volume dependences of δ_{CS} are similar to those of many ionic compounds [16]. At $\Delta V/V_0 \sim 0.13$, a large reduction in δ_{CS} of about 0.15 mm s^{-1} is observed in both FeS and Fe_7S_8, which shows a substantial change in the electronic structure of FeS and Fe_7S_8. The values of δ_{CS} above $\Delta V/V_0 \sim 0.13$ lie within the range of those of compounds with a highly covalent Fe(II) state: the low-spin Fe(II) state. We also obtain linear fits of the form

$$\delta_{CS} = (0.82 \pm 0.01) - (1.41 \pm 0.05)\Delta V/V_0 \text{ mm s}^{-1} \qquad \text{for FeS}$$

and

$$\delta_{CS} = (0.80 \pm 0.02) - (2.1 \pm 0.1)\Delta V/V_0 \text{ mm s}^{-1} \qquad \text{for } Fe_7S_8.$$

These coefficients of $\Delta V/V_0$ are much larger than those of ionic compounds and comparable with those of α-iron and other metallic compounds [17].

The experimentally observed variation of δ_{CS} with volume at constant temperature can be written in general as

$$\left[\frac{\partial \delta_{CS}}{\partial V}\right]_T = \left[\frac{\partial \delta}{\partial V}\right]_T + \left[\frac{\partial \delta_{SOD}}{\partial V}\right]_T .$$

The first term on the right-hand side represents the variation of the electron density at the nucleus and the second term describes the changes of the second-order Doppler (SOD) shift. Assuming a Grüneisen constant of 2 and using values of the Debye temperature, Θ_D, of 312 and 241 K for FeS and Fe_7S_8, respectively, obtained from the low-temperature specific heat measurements [9], the values of $\Delta\delta_{SOD}/(\Delta V/V_0)$ are estimated to be about +0.1 mm s^{-1} for FeS and +0.08 mm s^{-1} for Fe_7S_8. Since the volume effect on the SOD shift is small, the main effect in $[\partial\delta_{CS}/\partial V]_T$ must be caused by an increase of the electron density at the nucleus. Thus the volume reduction under pressure can be attributed to an increase in the degree of covalence in the S–Fe–S bonds, i.e. to an increase of the p–d hybridization.

The value of H_{hf} for FeS remains constant at 316 ± 3 kOe up to $\Delta V/V_0 = 0.055$ and decreases with increasing $\Delta V/V_0$ in the range from 0.055 to 0.11. In this range for FeS, a linear relation is found:

$$H_{hf} = (311 \pm 3) - (475 \pm 46)\Delta V/V_0 \text{ kOe}.$$

As seen in figure 4(b), the initial slope of H_{hf} versus $\Delta V/V_0$ for Fe_7S_8 is similar to that of the above relation. The value of H_{hf} at a finite temperature depends on the magnetic moment of an iron atom, the strength of the exchange interactions and the degree of covalence. As discussed in relation to the volume dependence of δ_{CS}, the degree of covalence increases with decreasing volume. In general, an increase in covalence contributes to a decrease of H_{hf} and changes a conversion coefficient between H_{hf} and the iron magnetic moment. In the cases for FeS and Fe_7S_8, however, the volume dependence of H_{hf} may directly relate to the sublattice magnetization of the iron sites, because an increase in covalence does not affect H_{hf} below $\Delta V/V_0 = 0.055$ for FeS. Since there is a pressure dependence of c/a for FeS and Fe_7S_8 [4], this produces not only the decrease of the Fe–S bond length but also the changes of the Fe–S–Fe bond angle and thus the volume dependence of the exchange interaction and the iron magnetic moment.

4.2. The electronic state under pressure

Below $\Delta V/V_0 = 0.055$ for FeS, the volume dependence of δ_{CS} is similar to those of ionic compounds and H_{hf} remains constant. A ^{129}I Mössbauer study on NiI_2 under pressure, which is a magnetic insulator, showed that the magnetic ordering temperature and δ_{CS} increase linearly with decreasing volume, and H_{hf} at 4.2 K is not affected by pressure

in the magnetic state [18]. In insulators without large volume reductions, the exchange interactions increase and the magnetic moment is not affected by the volume reduction. The result of the low-temperature specific heat measurement for FeS indicated that there is no discernible density of states at the Fermi energy within the accuracy of the data [9]. Since the structural phase transition occurs at T_α from the troilite to the NiAs structure [2], T_N for the troilite structure is impossible to determine exactly. However, the fact that there is no volume dependence of H_{hf} at room temperature suggests that T_N and the iron magnetic moment for the troilite structure could not decrease with this volume reduction. Therefore, it is concluded that the electronic state of FeS has an insulating character and the electrons on iron are well localized and thus contribute to the magnetic moment. This proposed electronic state is consistent with the results obtained by photoemission spectroscopy [10].

In the range from $\Delta V/V_0 = 0.055$ to 0.11 for FeS and below $\Delta V/V_0 = 0.13$ for Fe_7S_8, the volume dependence of δ_{CS} is similar to that of FeS below $\Delta V/V_0 = 0.055$, but H_{hf} decreases with the volume reduction. This large volume dependence of H_{hf} reflects the large decrease of magnitude of the iron magnetic moment and/or the strength of the exchange interactions. Since H_{hf} extrapolated to $\Delta V/V_0 = 0$ in FeS is almost same as the value below $\Delta V/V_0 = 0.055$, the magnetic properties are supposed not to be significantly different from those below $\Delta V/V_0 = 0.055$. According to the preliminary measurements of the pressure dependence of the electrical resistivity for FeS [19], it is found that the resistance decreases abruptly by about two orders of magnitude at 3.6 GPa and its temperature dependence is not like that of a simple metal in the phase with the MnP-type structure. Since the electronic state of FeS below $\Delta V/V_0 = 0.055$ is the insulating state as discussed above, and the volume reduction is attributed to the increase of bandwidth and the changes in the magnitudes of U and Δ, the gap in the electronic states decreases with decreasing volume. Thus the conduction band edge becomes lower in energy than the valence band edge at $\Delta V/V_0 = 0.055$ but the direct gap may not close up to $\Delta V/V_0 = 0.11$. Accordingly the electronic structure of FeS in this volume range is proposed to be like a semimetallic state. Because the crystal structure of Fe_7S_8 is different from that of FeS, there may be a difference between the electronic structures of Fe_7S_8 and FeS. However, it is suggested by the volume dependences of δ_{CS} and H_{hf} for Fe_7S_8 that there is an overlap in energy of the conduction and valence bands but the direct gap is still present. This overlap of the bands leads to an itinerant character of electrons and the strongly volume-dependent magnetic properties. As a result, anomalously small bulk moduli are observed in these phases. This proposed electronic structure could explain qualitatively the results for Fe_7S_8 obtained from the low-temperature specific heat measurements and the photoemission spectroscopy [9, 10].

The large decrease of δ_{CS} and the disappearance of H_{hf} at $\Delta V/V_0 \sim 0.13$ indicate a distinct change of the 3d-electron configuration on iron, and the volume dependence of δ_{CS} is comparable with those of metallic compounds above $\Delta V/V_0 \sim 0.13$ for FeS and Fe_7S_8. The previous high-pressure resistance measurement [20] indicated that FeS shows a slight increase in resistance with temperature in this phase. For ambient conditions, CoS with the NiAs-type structure is a Pauli paramagnetic metal [21] and the c-value is about 10% smaller than that of FeS and Fe_7S_8, and the electronic bandwidth is large enough for the state to become a metallic ground state, and there is a collapse of the magnetic moment of the cobalt atom. It was shown from the Mössbauer resonance of ^{57m}Fe atoms formed after the decay of ^{57}Co in CoS [22] that the spectrum consists of a quadrupole doublet and the value of δ_{CS} is 0.50 ± 0.05 mm s^{-1} at 295 K. This spectrum is similar to those of FeS and Fe_7S_8 in these volume ranges and the values of δ_{CS} are also in good agreement with those of FeS and Fe_7S_8. As the volume is decreased further, the overlap in bands increases and eventually the direct gap may go to zero. Although the vanishing of H_{hf} only implies that

there is no magnetic order at room temperature, these facts suggest that the spin splitting may be absent. Therefore it is proposed that a nonmagnetically metallic state like that of CoS appears to be suitable for describing the electronic states of FeS and Fe_7S_8 above $\Delta V/V_0 \sim 0.13$. This proposed nonmagnetically metallic state could explain qualitatively the large B-value.

5. Conclusion

The pressure-dependent phase diagrams of FeS and 3c-type Fe_7S_8 have been determined using ^{57}Fe Mössbauer spectroscopy and x-ray diffraction measurement only for Fe_7S_8. It is found from the Mössbauer spectroscopy that the transition takes place from magnetically ordered to nonmagnetic states at 6.5 and 4.5 GPa for FeS and Fe_7S_8, respectively, and that there is a large reduction in δ_{CS} at these pressures. It is shown by the x-ray diffraction measurements for Fe_7S_8 that there is a large increase in B and no discontinuous volume change at 4.5 GPa. A distinct steplike feature of H_{hf} for FeS is observed at 3.5 GPa with the change of spin direction.

The electronic state in each phase of FeS and Fe_7S_8 is proposed on the basis of the volume dependence of δ_{CS} and H_{hf}. In the low-pressure phase of FeS, the electronic state is an insulator and the electrons on the iron are well localized and thus contribute to a magnetic moment. In both the low-pressure phase of Fe_7S_8 and the intermediate-pressure phase of FeS, the electronic structure is deduced to be like a semimetallic state. The overlap in energy of the conduction and valence bands leads to the large volume dependence of their magnetic properties and hence the small bulk moduli. In the high-pressure phases of FeS and Fe_7S_8, the bandwidth is large enough for the state to become metallic. The large decrease of δ_{CS} and the disappearance of H_{hf} at $\Delta V/V_0 \sim 0.13$ indicate a distinct change of the 3d-electron configuration on the iron. It is suggested that the electron delocalization produces the collapse of the magnetic moment of the iron atom. It seems that the large increase in B at $\Delta V/V_0 \sim 0.13$ is caused by the transition from the magnetically semimetallic to the nonmagnetically metallic state.

Acknowledgments

We are grateful to Professors N Mori and H Takahashi for their kind advice on the setting up of a high-pressure x-ray diffraction apparatus. This work was partly supported by a Grant-in-Aid for Scientific Research from the Japanese Ministry of Education, Science and Culture.

References

[1] Zaanen J, Sawatzky G A and Allen J W 1986 *J. Magn. Magn. Mater.* **54–57** 607
[2] Horwood J L, Townsend M G and Webster A H 1976 *J. Solid State Chem.* **17** 35
[3] King H E Jr and Prewitt C T 1982 *Acta Crystallogr.* B **38** 1877
[4] Kamimura T, Sato M, Takahashi H, Mori N, Yoshida H and Kaneko T 1992 *J. Magn. Magn. Mater.* **104–107** 255
[5] King H, Virgo D and Mao H K 1978 *Carnegie Inst. Washington Yearbook* **77** 830
[6] Lotgering F K 1956 *Philips Res. Rep.* **11** 190
[7] Tokonami M, Nishiguchi K and Morimoto N 1972 *Am. Mineral.* **57** 1066
[8] Nakano A, Tokonami M and Morimoto N 1979 *Acta Crystallogr.* B **35** 722
[9] Kobayashi H, Nozue T, Matsumura T, Sato M, Suzuki T and Kamimura T 1997 to be published

[10] Shimada K, Mizokawa T, Saitoh T, Mamiya K, Fujimori A, Ono K, Kakizaki A, Ishii T, Shirai M and Kamimura T 1996 *J. Electron. Spectrosc. Relat. Phenom.* **78** 317
[11] Gosselin J R, Townsend M G and Tremblay R J 1976 *Solid State Commun.* **19** 799
[12] Theodosiou A 1965 *Phys. Rev.* **137** A1321
[13] Taylor R D and Pasternak M P 1990 *Hyperfine Interact.* **53** 159
[14] Toulmin P T and Barton P B 1964 *Geochim. Cosmochim. Acta* **28** 641
[15] Janak J F and Williams A R 1976 *Phys. Rev.* B **14** 4199
[16] Drickamer H G, Vaughan R W and Champion A P 1969 *Accounts Chem. Res.* **2** 40
[17] Pipkorn D N, Edge C K, Debrunner P, de Pasquali G, Drickamer H G and Frauenfelder H 1965 *Phys. Rev.* **135** A1604
[18] Pasternak M P, Taylor R D, Chen A, Meade C, Falicov L M, Giesekus A, Jeanloz R and Yu P Y 1990 *Phys. Rev. Lett.* **65** 790
[19] Kusaba K 1996 private communication
[20] Minomura S and Drickamer H G 1963 *J. Appl. Phys.* **34** 3043
[21] Kamimura T 1988 *J. Physique* **49** C8 191
It is found that the lower boundary of the CoS phase is located at about 51 at.% S, i.e., the homogeneity range does not include the stoichiometric composition and the CoS phase is unstable below ∼460 °C. See Rosenqvist T 1954 *J. Iron Steel Inst.* **176** 37
[22] Seregin P P, Bondarevskii S I and Efimov A A 1970 *Sov. Phys.–Solid State* **12** 1462